

# Determination of the Major Impurity Radiators in the Reheat Mode Discharges in the Compact Helical System

メタデータ	言語: eng 出版者: 公開日: 2011-03-07 キーワード (Ja): キーワード (En): 作成者: SUZUKI, Chihiro, AKIYAMA, Tsuyoshi, FUJISAWA, Akihide, IDA, Katsumi, ISOBE, Mitsutaka, MATSUOKA, Keisuke, MINAMI, Takashi, NAGAOKA, Kenichi, NISHIMURA, Shin, OKAMURA, Shoichi, PETERSON, Byron J., SHIMIZU, Akihiro, TAKAHASHI, Chihiro, TOI, Kazuo, YOSHIMURA, Yasuo メールアドレス: 所属:
URL	<a href="http://hdl.handle.net/10655/6333">http://hdl.handle.net/10655/6333</a>

# Determination of the Major Impurity Radiators in the Reheat Mode Discharges in the Compact Helical System

Chihiro SUZUKI, Tsuyoshi AKIYAMA, Akihide FUJISAWA, Katsumi IDA, Mitsutaka ISOBE, Keisuke MATSUOKA, Takashi MINAMI, Kenichi NAGAOKA, Shin NISHIMURA, Shoichi OKAMURA, Byron J. PETERSON, Akihiro SHIMIZU, Chihiro TAKAHASHI, Kazuo TOI and Yasuo YOSHIMURA

*National Institute for Fusion Science, Toki, Gifu 509-5292, Japan*

(Received 4 December 2006 / Accepted 12 March 2007)

Radiation brightness and impurity behaviors have been studied for reheat mode discharges in the Compact Helical System (CHS) by three different types of impurity diagnostics. Total radiation power measured by a pyroelectric detector significantly reduces after entering the reheat mode, whereas the line-averaged radiation brightness measured by an absolute extreme ultraviolet (AXUV) photodiode array increases especially for a center viewing chord due to the impurity accumulation in the plasma core. One possible reason for this opposite behavior between the two bolometric detectors is the reduced sensitivity of the AXUV photodiode for lower energy photons in vacuum ultraviolet (VUV) region. This speculation is supported by temporal evolutions of VUV spectra measured by a grazing incidence spectrometer. These results demonstrate that the comparison of three impurity diagnostics would be beneficial to the determination of the major impurity radiators and a comprehensive understanding of impurity behaviors in the reheat mode discharges.

© 2007 The Japan Society of Plasma Science and Nuclear Fusion Research

**Keywords:** CHS, reheat mode, impurity, bolometer, pyroelectric detector, AXUV photodiode, VUV spectrometer, spectral sensitivity

DOI: 10.1585/pfr.2.S1062

## 1. Introduction

Spatial and temporal behaviors of radiation and impurity ions in magnetically confined high temperature plasmas for fusion research are of great importance from the viewpoint of power balance and achievable plasma performance. In terms of the power balance, conventional thermal bolometric devices such as metal film and pyroelectric detectors have been used so far for the measurements of radiation brightness. A silicon device referred to as AXUV (absolute extreme ultraviolet) photodiode has also been used for bolometric measurements in fusion plasma experiments instead of the thermal devices [1, 2]. The AXUV photodiode is advantageous in that a simple and low-cost system can be constructed based on the silicon device though the spectral sensitivity is not completely uniform for low energy photons. On the other hand, spectroscopic measurements are indispensable to identify impurity ion species and study impurity generation and transport in plasmas. Spectrometers in the vacuum ultraviolet (VUV) wavelength region are widely used for fusion research since line radiation of VUV and soft X-ray photons is expected to be prominent in most experimental devices.

In the Compact Helical System (CHS), a medium-size helical device at the National Institute for Fusion Science (NIFS), three different types of impurity diagnostics men-

tioned above have been installed. Firstly, a pyroelectric detector is used for a total radiation power monitor as a conventional bolometer. In addition, an AXUV photodiode array has been installed to obtain profiles of radiation brightness. Finally, VUV spectra have been measured by a grazing incidence spectrometer.

In this article, we report the results of radiation and impurity measurements for reheat mode discharges [3, 4] in CHS measured by these diagnostics since the different features of the three types of diagnostics are well demonstrated in this discharge. Namely, the total radiation power measured by the pyroelectric detector shows opposite behavior to the AXUV photodiode signals during the reheat mode. The reason for this behavior and the major impurity radiators are discussed based on the comparisons with the VUV spectra in connection with the spectral sensitivity of the AXUV photodiode.

## 2. Diagnostics

The CHS is a low-aspect-ratio medium-size helical device whose average major and minor radii are 1 and 0.2 m, respectively. Figure 1 (a) shows a top view of the arrangement and the viewing angles of the impurity diagnostics equipped in CHS. A single channel pyroelectric detector (Molelectron, P1-12) is used for routine monitoring of the total radiation power from the plasma with a wide

author's e-mail: csuzuki@lhd.nifs.ac.jp

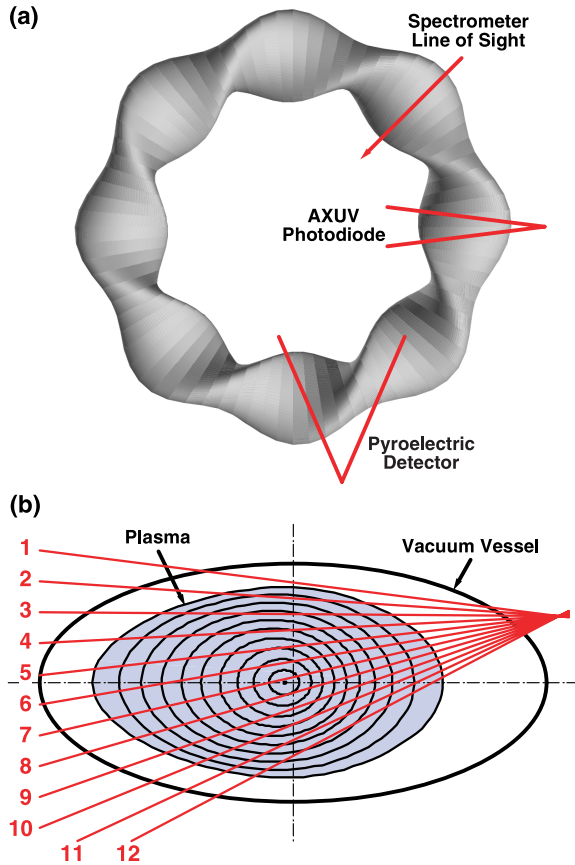


Fig. 1 (a) Top view of the arrangement and the viewing angles of the impurity diagnostics in CHS. (b) The lines of sights of the AXUV photodiode array and the flux surfaces of a plasma with magnetic axis position of  $R_{ax} = 93.5$  cm and an average beta of 0.5 %.

viewing angle. The lines of sights of the AXUV photodiode array (IRD, AXUV-20EL) have been arranged within a horizontally elongated cross section as shown in Fig. 1 (b) in which the flux surfaces for the magnetic configuration used in this study are superposed. Because of the limitation of the data acquisition system, only 12 channels out of 20 can be measured simultaneously. A compact mounting module including an in-vacuum preamplifier has successfully been designed and fabricated for the photodiode array [5].

For the survey of VUV spectra and monitor of impurity spectral line intensities, we have utilized a flat field grazing incidence spectrometer (Shinku-Kogaku, model JYF-306) with a focal length of 306 mm. The detailed specification of the spectrometer has already been reported elsewhere [6]. The wavelength range and the spectral resolution of the spectrometer are 10-110 nm and 0.3 nm, respectively. The line of sight of the spectrometer is fixed at a line passing through the plasma center within a horizontally elongated cross section. Time evolutions of the impurity line intensities can be obtained in a single shot at

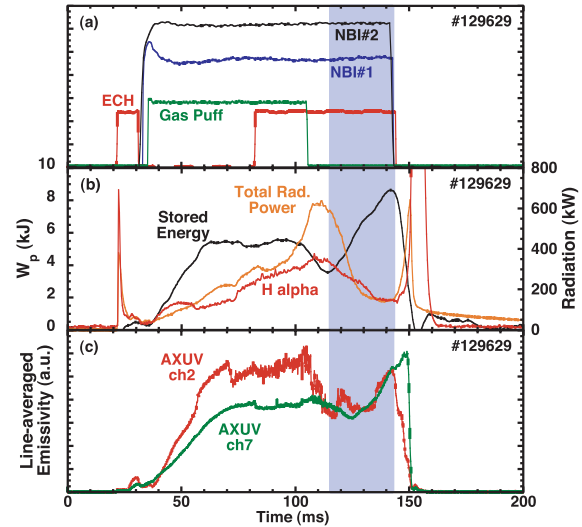


Fig. 2 Temporal evolutions of various parameters in a reheat mode discharge ( $R_{ax} = 93.5$  cm). The reheat mode is kept during 115-145 ms. (a) Timings of the heating and gas puff, (b) stored energy, total radiation power, and  $H_\alpha$  intensity, (c) AXUV photodiode signals averaged along the lines of sights of channel 2 and 7 shown in Fig. 1 (b).

10 ms intervals which is limited by the minimum readout time of a linear image sensor.

### 3. Reheat Mode

An improvement of the stored energy due to the reheat mode has been observed after the termination of the intense gas puffing in high density CHS plasmas as described in the previous articles [3,4]. Recently the maximum plasma stored energy of CHS has been explored by the reheat mode under the highest magnetic field strength ( $\approx 1.8$  T) and the maximum neutral beam (NB) heating power ( $\approx 1.7$  MW). The maximum stored energy of 9.4 kJ has consequently been achieved in the magnetic axis position  $R_{ax} = 94.9$  cm (in major radius) [4]. However, another reheat mode discharge with  $R_{ax} = 93.5$  cm is adopted as a representative shot in this study since all of the impurity diagnostics were in operation in this shot.

The temporal evolutions of the several parameters for the representative reheat mode discharge with  $R_{ax} = 93.5$  cm are summarized in Fig. 2. The discharge is initiated by electron cyclotron heating (ECH) followed by dual co-injected NB heating with a total power of 1.7 MW. Although the second ECH is applied from 80 ms for another purpose, it does not affect the features of the reheat phase and the resulting phenomena. A strong gas puff is injected during 35-105 ms which results in the maximum line-averaged electron density of about  $1.2 \times 10^{20} \text{ m}^{-3}$  (not shown in Fig. 2) just after the termination of the gas puff. The total radiation power monitored by the pyroelectric detector steeply increases as the electron density approaches

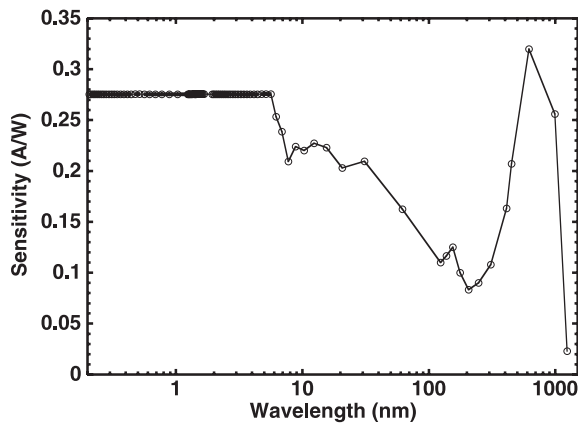


Fig. 3 The spectral dependence of the sensitivity of the AXUV photodiode.

the upper limit. Although the stored energy decreases from 100 ms due to the increase in the total radiation power, it recovers from 115 ms (10 ms after the termination of the gas puff) by entering the reheat mode, and finally reaches up to 8.6 kJ at 142 ms. According to the electron temperature profiles measured by the Thomson scattering diagnostic, the electron temperature at 140 ms (after the reheat) increases by 100–150 eV through the whole area of the plasma in comparison with that at 105 ms (before the reheat), which largely contributes to the increase in the stored energy during the reheat mode. The central electron temperature at 105 and 140 ms are about 280 and 430 eV, respectively.

The AXUV photodiode signals for the edge (channel 2) and the center (channel 7) viewing chords are displayed in Fig. 2 (c). The minimum normalized minor radii for the edge and center chords are 0.87 and 0.04, respectively, for the plasma shown in Fig. 1 (b). The temporal behaviors of the AXUV photodiode signals during the reheat mode was obviously different from that of the total radiation power. Namely, the total radiation power measured by the pyroelectric detector significantly reduces during the reheat mode, whereas the AXUV photodiode signals increase especially for the center viewing chord. The results of the previous studies on the reheat mode implies the accumulation of impurity ions into the plasma core during the reheat mode [3]. Therefore the steep increase in the AXUV photodiode signals in Fig. 2 (c) possibly represent the impurity accumulation. However, the effect of this phenomenon is hardly observed in the signal of the pyroelectric detector.

One possible reason for this opposite behavior between the two bolometric detectors would be the spectral dependence of the sensitivity of the AXUV photodiode shown in Fig. 3, where the data provided by the manufacturer is plotted as a function of wavelength. The reduction of the sensitivity due to the absorption inside the thin oxide layer on the surface of the bulk silicon is observed in wavelength longer than 6 nm, and it decreases

until 200 nm. Furthermore, the sensitivity degradation in this region is anticipated during the long-term exposure to the strong emissions from the plasmas, judging from the present experimental data. Therefore the AXUV photodiode may become almost blind to relatively low energy photons emitted mainly from the plasma edge, where the electron temperature is relatively low (below 100 eV). The validity of this speculation is discussed in more detail in the next section by comparing with the temporal evolutions of VUV spectra.

A spontaneous drop and a recovery of hydrogen Balmer alpha ( $H_{\alpha}$ ) emission intensity observed at 55 and 75 ms are due to the transition to and the back transition from the edge transport barrier (ETB) phase, which has been described elsewhere [7–10]. The buildup of the edge AXUV signal (channel 2) observed during 55–75 ms is caused by the formation of the ETB [8].

#### 4. Comparison with VUV Spectra

In order to assess the speculation in the previous section, temporal evolutions of the VUV spectra were measured at 10 ms intervals in the same reheat mode discharge. The spectra in 10–85 nm region observed for the same shot as Fig. 2 are shown in Fig. 4 (a) for three timings. The exposure time of the spectrometer for each spectrum is 10 ms. Several resonance lines of metallic (iron, chromium, titanium) and non-metallic (oxygen) impurities have been identified from the measured spectra as indicated in Fig. 4 (a). The metallic impurity lines mainly appear in the shorter wavelength region below 50 nm, whereas oxygen lines appear in the longer wavelength region. By comparing the spectra at 65 and 105 ms, it is clearly seen that the emissions only in the longer wavelength region become brighter at 105 ms than at 65 ms. In the reheat phase at 145 ms, on the other hand, the shorter wavelength region becomes bright and the longer wavelength region weak. This different behavior between the two wavelength region are more clearly represented in Fig. 4 (b), where temporal evolutions of several representative impurity lines are plotted at 10 ms intervals. All of the line intensities are normalized at 55 ms taking account of the spectral dependence of the spectrometer sensitivity. Before the reheat phase, the emission from highly charged metallic ions saturates at 65 ms, while the emission from relatively low charged oxygen ions continues to increase until the termination of the gas puff at 105 ms. In contrast, the former largely increases in the reheat mode, and the latter steeply decreases until 135 ms and increases again at 145 ms.

By comparing Fig. 2 and Fig. 4 (b), it can be said that the behaviors of the metallic impurity lines agree well with those of the AXUV photodiode signal of the center chord, while the behaviors of the oxygen lines are similar to the total radiation power. Judging from the ionization energies of these ions, the former and the latter are emitted from the

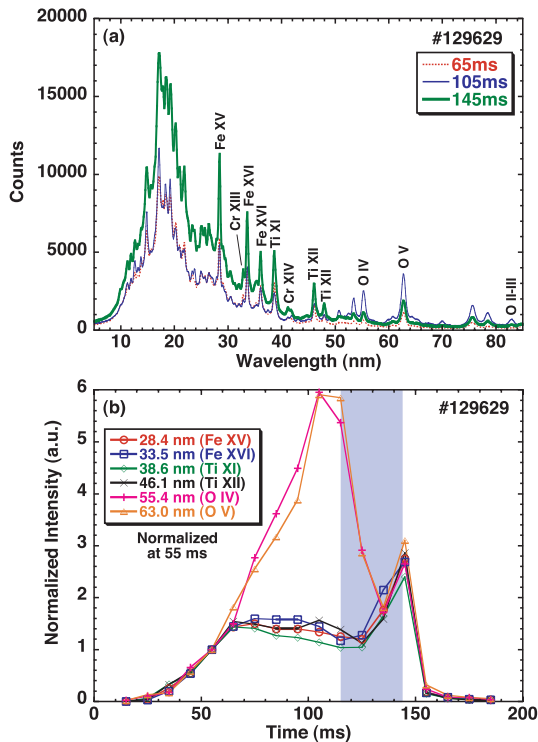


Fig. 4 (a) VUV spectra observed in the same reheat mode discharge as Fig. 2 for three timings. The exposure time of the spectrometer for each spectrum is 10 ms. The spectra in the gas puff phase (65 ms), just before the reheat phase (105 ms), and during reheat phase (145 ms) are displayed with the identified impurity emission lines. (b) Temporal evolutions of iron, titanium and oxygen line intensities normalized at 55 ms.

core and the edge plasmas, respectively. Therefore these observations imply that the metallic impurities accumulate into the plasma core during the reheat mode, and the radiation from the edge plasma becomes dominant before entering the reheat mode though it cannot be observed by the AXUV photodiode. The impurity accumulation occurred locally in the core does not appear in the total radiation power since the volume of the edge plasma is much larger than that of the core plasma. This result strongly supports the speculation in the previous section that the opposite behavior between the two bolometric detectors could be at-

tributed to the difference in the spectral sensitivity in the VUV region.

## 5. Conclusion

We have measured radiation brightness and impurity emission lines for the reheat mode discharges in CHS by three different types of diagnostics. Opposite behaviors between the two bolometric detectors were observed during the reheat mode, which could be attributed to differences in the spectral sensitivity in the VUV region, which is validated by the observations of the VUV spectra. This study indicates that special care about the spectral sensitivity should be taken in the analyses of the AXUV photodiode in comparison with conventional bolometers, especially in plasmas where the radiations of low energy photons may become dominant. The total radiation power monitored by the pyroelectric detector seems to be dominated by emission from light impurities like oxygen ions in the low temperature edge region of the plasma. The comparison among three types of impurity diagnostics which have different characteristics utilized in this study are helpful for the determination of the major impurity radiators and a comprehensive understanding of overall impurity behavior in magnetically confined high temperature plasmas.

- [1] R.L. Boivin, J.A. Goetz, E.S. Marmar, J.E. Rice and J.L. Terry, *Rev. Sci. Instrum.* **70**, 260 (1999).
- [2] Y. Liu, A. Yu. Kostrioukov, B.J. Peterson and LHD Experiment Group, *Rev. Sci. Instrum.* **74**, 2312 (2003).
- [3] S. Morita *et al.*, *Proc. 14th Int. Conf. Plasma Physics and Controlled Nuclear Fusion Research 1992*, Würzburg, 1992, Vol.2, p.515.
- [4] M. Isobe *et al.*, *Fusion Sci. Technol.* **50**, 229 (2006).
- [5] C. Suzuki, B.J. Peterson and K. Ida, *Rev. Sci. Instrum.* **75**, 4124 (2004).
- [6] C. Suzuki *et al.*, *J. Plasma Fusion Res. SERIES* **7**, 73 (2006).
- [7] S. Okamura *et al.*, *Plasma Phys. Control. Fusion* **46**, A113 (2004).
- [8] C. Suzuki *et al.*, *Proc. 33rd EPS Conf. on Plasma Phys.*, Rome, 19-23 June 2006 ECA **30I**, P-4.120 (2006).
- [9] T. Minami *et al.*, *Plasma Fusion Res.* **1**, 032 (2006).
- [10] T. Akiyama *et al.*, *Plasma Phys. Control. Fusion* **48**, 1683 (2006).